

NASA TECHNICAL NOTE



NASA TN D-5925

c. 1

NASA TN D-5925

LOAN COPY: RETURN
AFWL (WL0L)
KIRTLAND AFB, N

01322705



TECH LIBRARY KAFB, NM

TRANSIENT CHARACTERISTICS OF
A VOLTAGE REGULATOR AND
A PARASITIC SPEED CONTROLLER ON
A 14.3-KILOVOLT-AMPERE, 1200-HERTZ
MODIFIED LUNDELL ALTERNATOR

by Heinz L. Wimmer and Bill D. Ingle

Lewis Research Center

Cleveland, Ohio 44135



0132705

1. Report No. NASA TN D-5925	2. Government Accession No.	3. Recipient's Catalog No.	
4. Title and Subtitle TRANSIENT CHARACTERISTICS OF A VOLTAGE REGULATOR AND A PARASITIC SPEED CONTROLLER ON A 14.3-KILOVOLT-AMPERE, 1200-HERTZ MODIFIED LUNDELL ALTERNATOR		5. Report Date October 1970	6. Performing Organization Code
7. Author(s) Heinz L. Wimmer and Bill D. Ingle	9. Performing Organization Name and Address Lewis Research Center National Aeronautics and Space Administration Cleveland, Ohio 44135	8. Performing Organization Report No. E-5626	10. Work Unit No. 120-27
12. Sponsoring Agency Name and Address National Aeronautics and Space Administration Washington, D.C. 20546	11. Contract or Grant No.		13. Type of Report and Period Covered Technical Note
15. Supplementary Notes	14. Sponsoring Agency Code		
16. Abstract The transient performances of a voltage regulator and a parasitic speed controller on a turbine-driven alternator were determined experimentally. The voltage regulator and the speed controller were developmental components for use in a 10-kilowatt, 1200-hertz Brayton-cycle space power generating system. Voltage excursions, voltage recovery times, and frequency recovery times were well within design goals. Frequency excursions exceeded the design goal by a small amount.			
17. Key Words (Suggested by Author(s)) Electrical system; Power generation; Electric controls; Alternator; Voltage regulator; Speed controller	18. Distribution Statement Unclassified - unlimited		
19. Security Classif. (of this report) Unclassified	20. Security Classif. (of this page) Unclassified	21. No. of Pages 26	22. Price* \$3.00

TRANSIENT CHARACTERISTICS OF A VOLTAGE REGULATOR AND A PARASITIC
SPEED CONTROLLER ON A 14.3-KILOVOLT-AMPERE,
1200-HERTZ MODIFIED LUNDELL ALTERNATOR

by Heinz L. Wimmer and Bill D. Ingle

Lewis Research Center

SUMMARY

The transient performances of a voltage regulator and a parasitic speed controller for the 10-kilowatt, 1200-hertz Brayton-cycle space power system were evaluated. An air-driven facility turbine and a research alternator were used. The alternator was an electromagnetic equivalent of the alternator used in the Brayton system.

The testing consisted of the step application and removal of useful load with the alternator producing rated output power in the steady state. The voltage regulator was evaluated in terms of peak voltage excursions and voltage recovery times. The speed controller was evaluated in terms of speed overshoot, undershoot, and recovery time. In order to investigate the performance of the speed controller and the buildup of voltage relying on residual magnetism, a full-power startup was performed.

For the useful-load transient tests performed, the maximum voltages were less than 124 percent of rated voltage. The voltage recovery times were less than 0.08 second. The response of the speed controller varied from an overdamped to an underdamped characteristic over the range of useful loads stepped. For a rated useful-load removal, the speed overshoot the steady-state regulation band; it returned to the band in 0.34 second. The system tested was stable. The full-power startup resulted in rated operating conditions being achieved in 3.5 seconds. The frequency overshoot was 0.56 percent. The voltage reached its rated value at 72 percent of rated speed.

INTRODUCTION

The transient performances of a voltage regulator and a parasitic speed controller on a turbine-driven alternator were determined experimentally. The voltage regulator and the speed controller were developmental components for use in the 10-kilowatt,

1200-hertz Brayton-cycle space power generating system (ref. 1). These components were assembled in the Electrical Control Package (ECP), which was designed for operation in a vacuum (ref. 2).

Speed control is accomplished by controlling the input-output power balance of the system. In order to maintain an essentially constant alternator load, the speed controller adjusts the parasitic load as the useful load is varied. Speed controllers of this type were used in the Sunflower, SNAP-2, SNAP-8, and 400-hertz Brayton-cycle space power systems (refs. 3 to 9).

The useful-load rating for the system is 10 kilowatts at 0.85 lagging power factor. The alternator rating is 14.3 kilovolt-amperes or 10.7 kilowatts at 0.75 lagging power factor. The major testing consisted of the step application and removal of a range of useful loads with the alternator producing 10.7 kilowatts in the steady state. The resultant voltage and frequency transients are described in terms of percent overshoot, percent undershoot, and recovery times. A discussion is presented relating the response of frequency (i.e., whether the response is overdamped or underdamped) to the incremental gain of the speed controller. Next, a determination of parasitic load margin is presented. This margin is the value of parasitic load required at rated useful load to prevent the loss of control of speed upon the step application of rated useful load. Finally, plots of voltage, speed, and field currents are presented to illustrate the performance of the controls during a startup relying on the residual magnetism of the alternator.

The alternator for the Brayton system is located on a shaft in common with a turbine and a compressor. This assembly operates at 36 000 rpm on gas bearings. It is referred to as the Brayton Rotating Unit or BRU. For component testing, a magnetic equivalent of the alternator, but with ball bearings, was fabricated and tested (ref. 10). For the testing at Lewis, this alternator was driven by a facility air turbine. The polar moment of inertia of this turbine-alternator combination differed from the rotational inertia of the BRU. For these tests the compressor was not simulated.

DESCRIPTION OF TEST SYSTEM

Components

A block diagram representation of the system tested is shown in figure 1. Instrumentation points are indicated on the figure. The major components of the system are the turbine, the alternator, and the Electrical Control Package (ECP). The ECP consists of a voltage regulator and a parasitic speed controller. The voltage regulator consists of the shunt field regulator and the series field controller. The turbine, alternator, and ECP in the test facility are shown in figure 2.

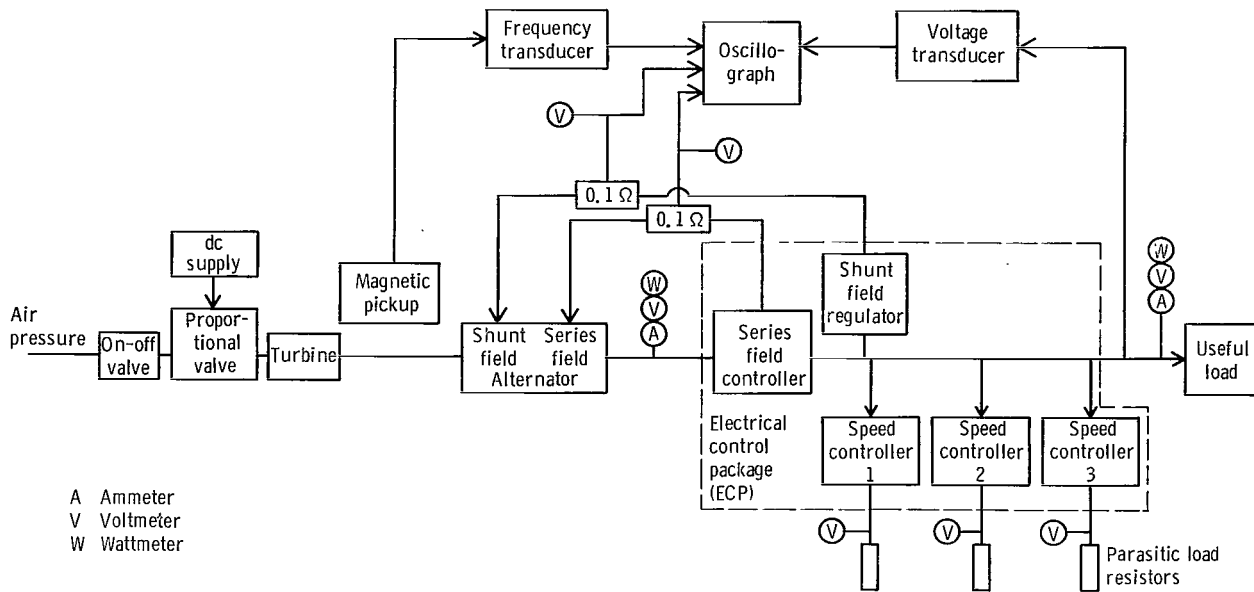


Figure 1. - Apparatus and instrumentation.

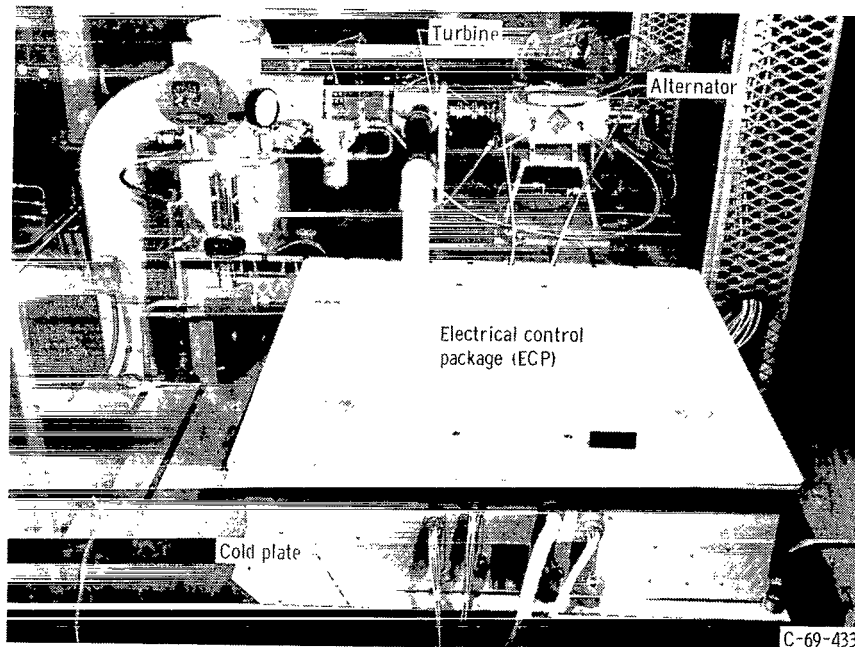


Figure 2. - Test apparatus for 1200-hertz Brayton electrical system.

The ECP was designed for vacuum operation. Cooling is provided by a cold plate. For the tests performed the coolant was water, which could be heated by means of an immersion heater in the water line. The temperature of the cold plate was maintained within $\pm 2^{\circ}$ C of 25° C.

Turbine. - The turbine is designed to produce 16 horsepower (11.9 kW) at 36 000 rpm at an air pressure drop of 12 psi (0.83×10^5 N/m²) and 80 horsepower (59.5 kW) at 40 psi (2.76×10^5 N/m²). The maximum design inlet-air temperature is 65° C. The turbine is of the radial flow design. The polar moment of inertia of the turbine-alternator combination is 0.039 in.-lb-sec² (4.4×10^{-3} kg-m²). For the BRU, the polar moment of inertia is 0.058 in.-lb-sec² (6.5×10^{-3} kg-m²). For the testing reported herein, the compressor was not simulated.

The frequency transients obtained in this test system will differ from those obtained for the Brayton system. However, the difference in the transient performances of the two systems can be approximately related through the ratio of their time constants. The ratio of the time constants is equal to the ratio of the moments of inertia.

Alternator. - The alternator is a solid-rotor modified-Lundell machine. It is rated at 14.3 kilovolt-amperes, 0.75 lagging power factor, 120/208 volts, three phase, and 1200 hertz at 36 000 rpm. The alternator has two stationary field windings (series and shunt fields) for voltage control.

Design data and features for this alternator are presented in references 11 and 12. Experimental results of the alternator saturation, efficiency, harmonic analysis, voltage unbalance, machine reactances, and time constants are presented in reference 10.

Voltage regulator. - Series excitation for the alternator is provided by the series field controller. A diagram of this controller is shown in figure 3. It consists of three

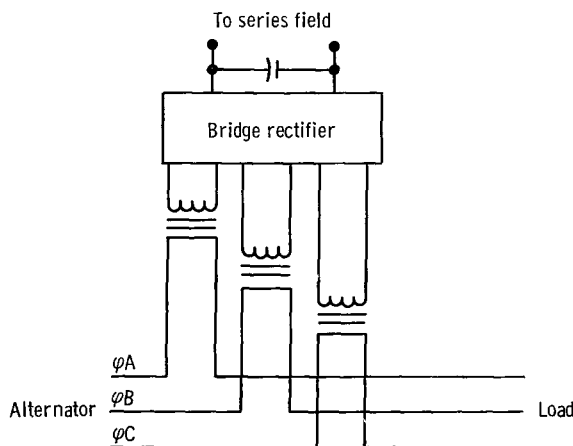


Figure 3. - Series field controller. Primary windings consist of one turn.

single-phase current transformers, a full-wave rectifier bridge, and filter capacitors. The output current of the series field controller is directly proportional to armature current.

The additional excitation required to maintain constant voltage is provided by the shunt field regulator. A block diagram of this regulator is shown in figure 4. The power supply provides a regulated voltage for the several transistor amplifiers and an unregulated voltage for the field. The output of the voltage sensor is compared with the reference voltage. If this output is greater than the reference, the error detector drives the

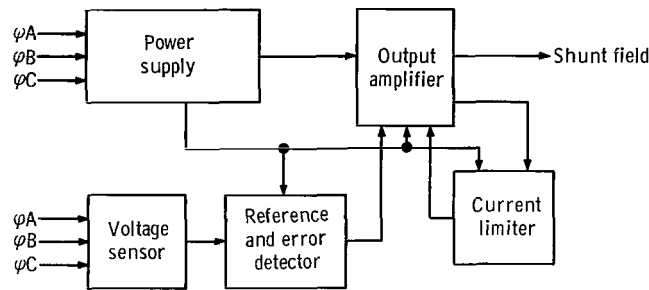


Figure 4. - Shunt field regulator.

output amplifier, resulting in a decrease in the shunt field current. The current limiter holds the field current to a maximum preset value. Detailed description of the operation of the voltage regulator is given in references 11 and 13.

Parasitic speed controller. - The speed controller applies or removes parasitic load to maintain the design frequency range as the useful load and alternator input conditions vary. A block diagram of the speed controller is shown in figure 5. Three channels are used; each senses the frequency on one phase of the alternator to provide redundancy. And each channel loads all three phases simultaneously. The maximum parasitic load capacity per phase for one channel is 2 kilowatts, giving a total of 6 kilowatts per channel. As the maximum parasitic load required to maintain speed is 10.7 kilowatts, one channel may fail in the off condition without affecting total alternator loading capability.

Each channel consists of a frequency detector, a preamplifier, an amplifier, and a firing circuit. The frequency detector converts the frequency error to a direct-current (dc) signal. This signal is amplified by two stages of push-pull magnetic amplifiers. The output of the magnetic amplifiers is proportional to the frequency error. This output determines the time to saturation of the reactor. Saturation of the reactor causes the silicon controlled rectifier (SCR) to conduct. Detailed description of the operation of the speed controller is given in references 11 and 13.

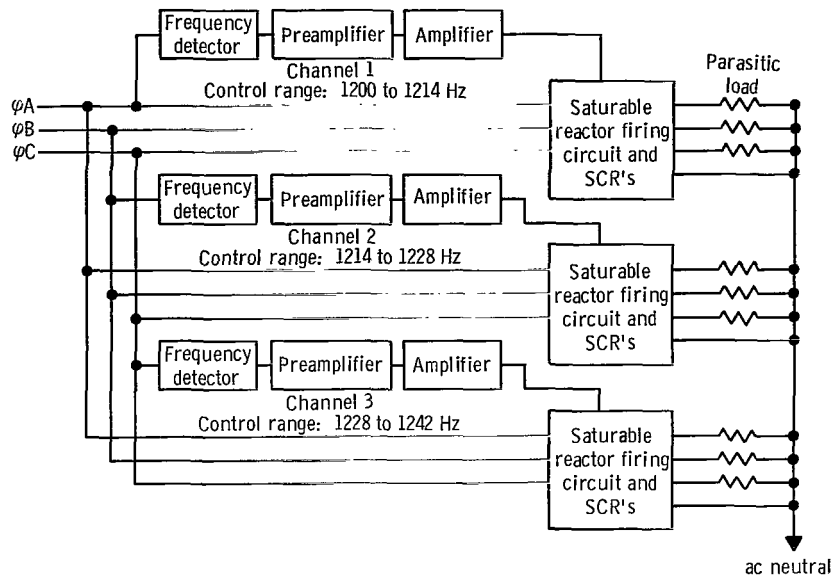


Figure 5. - Speed controller. Each resistor dissipates 2 kilowatts at 120 volts (line-to-neutral).

Instrumentation

The major steady-state parameters measured included (1) useful-load voltage, (2) electrical frequency, (3) line current, (4) power output, and (5) field currents. Measurements were made of transient useful-load voltage, frequency, and field currents. The outputs of the transducers were recorded by means of a light-beam oscillograph. Galvanometers used were of the fluidic-damped type and had a natural undamped resonant frequency of 1650 hertz or greater with a linearity of 2 percent.

Figure 6 is a schematic diagram of the voltage transducer used. The three-phase full-wave rectifier provides a dc signal proportional to the envelope of the line voltage.

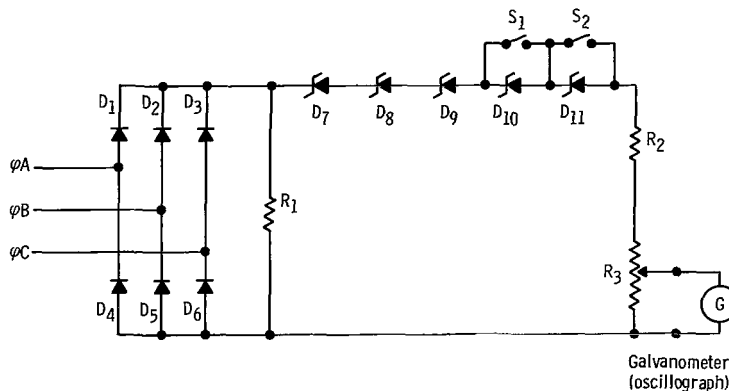


Figure 6. - Voltage transducer.

The zener diodes subtract a constant dc voltage to allow greater amplification of the range of interest. This circuit has minimal reactance to give accurate transient response. Additional description is given in reference 14.

The frequency transducer is a commercial instrument which produces a constant-width pulse for each cycle of the input frequency. The pulse is filtered by means of the output impedance of the transducer and a capacitor connected externally. This filtering results in a dc signal proportional to input frequency. In order to detect small changes in frequency, this dc signal is compared with an adjustable reference signal and the difference is amplified before being applied to the oscillograph.

Alternator field currents were obtained by directly recording the voltage signal of 0.1-ohm shunts connected in series with the fields. Additional instrumentation was used in establishing the steady-state loads. The specifications and uses of the instruments are given in table I.

TABLE I. - INSTRUMENT SPECIFICATIONS

Instrument	Use	Range	Accuracy	Additional specifications
True rms voltmeter	Line voltage	0 to 150 V	0.25 percent of full scale	Accuracy: to 2500 Hz
Wattmeter	Power	Nominal input: 100 V, 5 A	1 percent of full scale	Accuracy: dc to 2500 Hz
Current transformer	Line currents	Current ratio: 10:1	±0.1 percent of ratio	Accuracy: 70 to 2500 Hz; capacity: 25 V-A
Shunt	Secondary of current transformer, field currents	Resistance: 0.1 Ω	0.04 percent (in air)	Capacity: 15 A
True rms-to-dc converter	rms voltage on shunts	Input: 0 to 1 V Output: 0 to 10 V	0.1 percent of full scale	Accuracy: 40 to 3×10^4 Hz
Integrating digital voltmeter	Output of true rms-to-dc converter	0 to 15 V	0.1 percent (±1 digit)	-----
Millivoltmeter	Voltage of field current shunts	{0 to 200 mV} {0 to 500 mV}	0.25 percent of full scale	-----
Oscilloscope	Peak line voltage	100 V/cm	Deflection: 3 percent	-----
Temperature recorder	ECP cold plate temperature	200 to 650 K	±1 K	-----
Counter	Line frequency	0 to 9999.9 Hz	±0.1 Hz	-----

Procedure

For all but one of the tests, steady-state alternator output power was maintained at the rated value of 10.7 kilowatts. Balanced three-phase useful load was varied in increments of 1 kilowatt between 0 and 10 kilowatts at 1.0 and 0.85 power factor (lagging).

After the useful load of interest was set up, all the instruments were read. These results are presented and analyzed in reference 13. This useful load was then removed and reapplied, with the variables mentioned earlier being recorded on the oscillograph.

RESULTS AND DISCUSSION

The line-to-neutral voltage, frequency, and field currents for a 10-kilowatt, 0.85-lagging-power-factor useful-load application and removal are shown in figures 7 and 8.

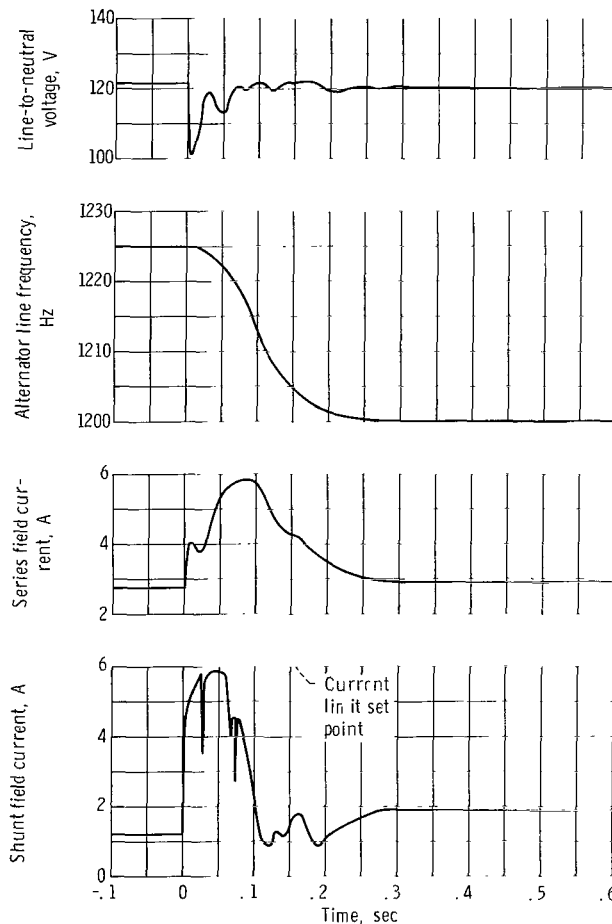


Figure 7. - Response to a step application of 10-kilowatt, 0.85-power-factor (lagging) useful load.

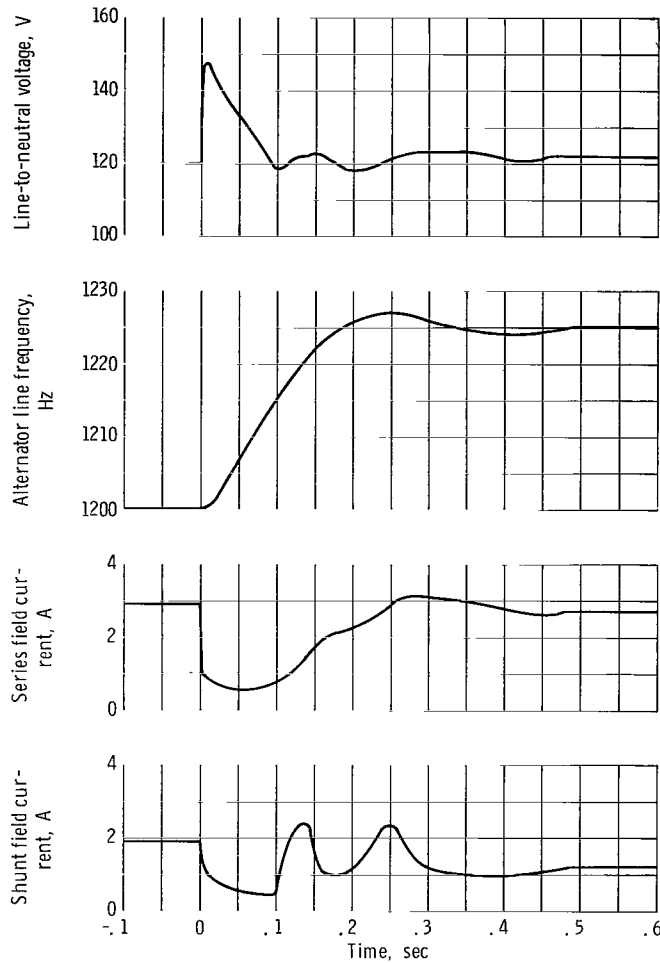


Figure 8. - Response to step removal of 10-kilowatt, 0.85-power-factor (lagging) useful load.

These curves were transcribed from the oscillographic recording.

In figure 7 the response to the step application of rated useful load is shown. As the voltage drops, the shunt field current rises immediately to the current limit range, thus providing a degree of field-forcing which should give a minimal voltage recovery time. The response of frequency is characteristic of an overdamped second-order system (ref. 15). The difference between the initial and final values of the variables results from the change in alternator loading conditions. This difference is discussed in detail in reference 13. The sharp dips in the shunt field current trace are caused by the voltage entering and leaving the steady-state regulation range.

The response to the step removal of load is shown in figure 8. The voltage overshoots the regulation range, causing the voltage regulator to turn off and the shunt field current to decay. Since there is no forcing action by the regulator, the voltage takes

TABLE II. - ELECTRICAL SYSTEM DESIGN GOALS

Voltage:	
Rated (E_R), V_{L-N}	120
Regulation, percent E_R	± 1
Recovery time ($\Delta E \leq \pm 5$ percent E_R), sec	0.25
Transient (max.), percent E_R	136
Frequency:	
Rated (F_R), Hz	1200
Regulation, percent F_R	± 1
Recovery time ($\Delta F \leq F_{\text{steady state}} \pm 2$ Hz), sec	1
Transient (max.), percent F_R	± 2
Modulation, Hz	± 2
Power rating:	
Alternator output (at 0.75 PF lagging), kW	10.7
Useful load (at 0.85 PF lagging), kW	10

longer to recover than for the load application case. The response of frequency is characteristic of an underdamped second-order system.

The voltage and frequency transients obtained over the range of useful-load transients are described in the following sections. Steady-state and transient design goals for the electrical system are listed in table II.

Voltage Transients

With reference to figure 9, the following terms are defined:

$$\frac{V_{L-N} + \Delta V}{120} \times 100 \quad \text{maximum (or minimum) voltage, percent of rated}$$

T_R voltage recovery time: the time for the voltage to return to and remain within ± 5 percent of 120 volts, sec

T_S voltage settling time: the time for the voltage to reach and remain within ± 1 percent of the final voltage, sec

The maximum and minimum voltages obtained for load removals and load applications are shown in figure 10. The largest voltage excursion occurred for a 10-kilowatt, 0.85-lagging-power-factor useful-load removal. The maximum voltage obtained for this

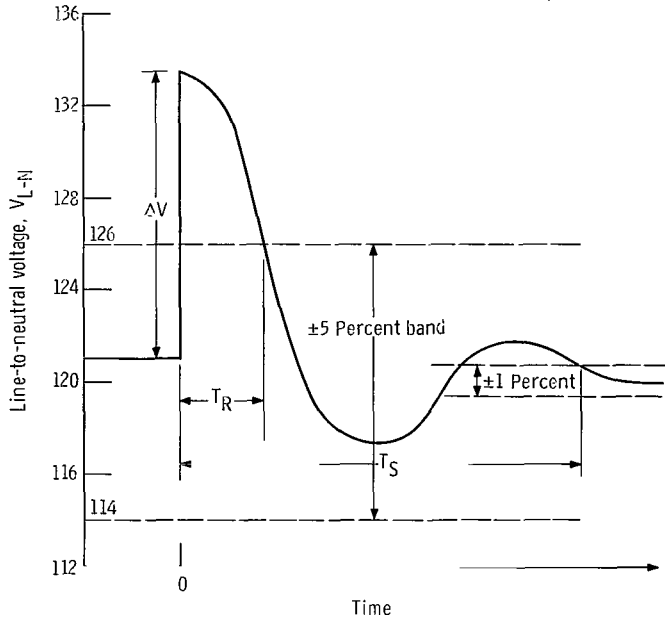


Figure 9. - Definition of parameters used in describing voltage transients.

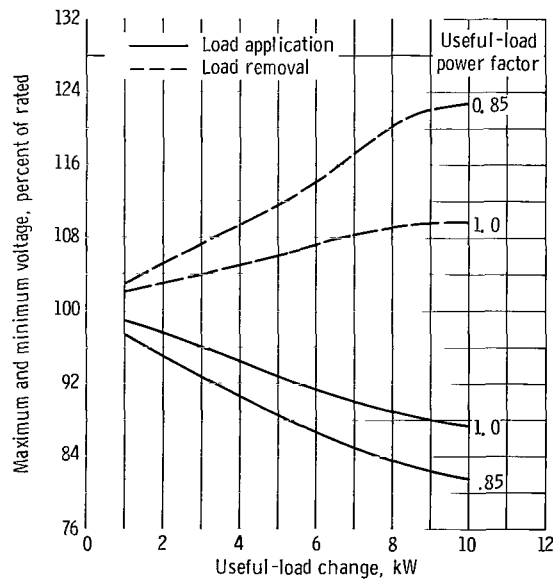


Figure 10. - Maximum and minimum voltage for step useful-load changes.

step change was 123 percent, which is well below the 136 percent design goal. The power factors given in figure 10 are for the useful load. The total alternator load power factor is considerably different; it is a function of the reactive loading effects of the speed controller and the reactive loading of the useful load. Additional discussion is given these effects in references 13 and 16.

Voltage recovery time as a function of step useful-load change is presented in figure 11. For useful-load transients up to and including 3 kilowatts, the voltage remained within the ± 5 percent band. Therefore, for this range, the recovery time is zero. The largest value of recovery time occurred for an 8-kilowatt, 0.85-power-factor useful-load removal. The value obtained for this transient was 0.074 second, which is much less than the 0.25-second design goal.

Values of recovery time for load applications are much less than for load removals. The difference is due to the field-forcing provided by the voltage regulator when, upon application of load, the line voltage drops. Upon load removal, the voltage rises out of the regulation range and results in the regulator turning off. The field currents then decay as determined by the time constants of the system.

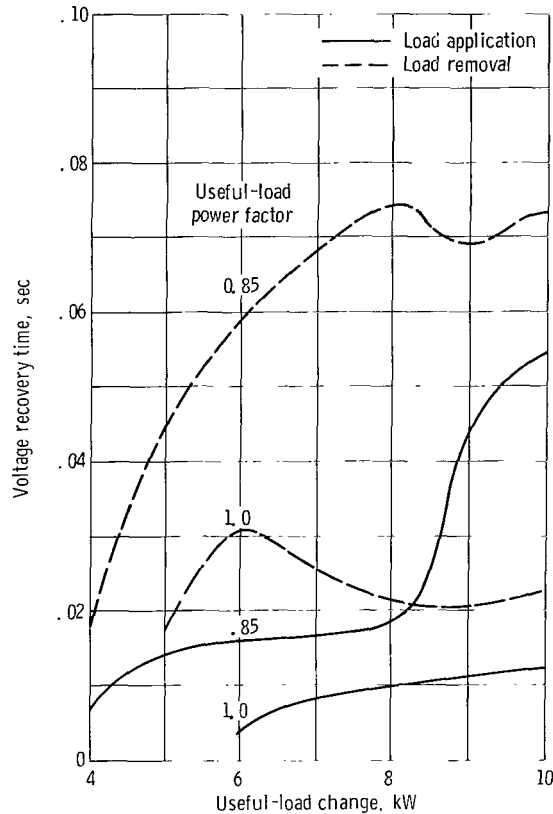


Figure 11. - Voltage recovery time for step useful-load changes.

TABLE III. - VOLTAGE SETTling TIME FOR
STEP USEFUL-LOAD CHANGES

Power factor	Useful load, kW	Load application settling time, ^a sec	Load removal settling time, sec
1.0	1	0.092	0.096
	2	.128	.158
	3	.111	.187
	4	.176	.162
	5	.201	.285
	6	.224	.209
	7	.390	.206
	8	.209	.213
	9	.208	.221
	10	.253	.364
0.85	1	0.073	0.103
	2	.117	.166
	3	.103	.186
	4	.081	.169
	5	.218	.201
	6	.199	.291
	7	.395	.297
	8	.216	.211
	9	.199	.361
	10	.212	.368

^aSettling time is defined as the time for the voltage to enter and remain within a ± 1 percent band of its final value.

Voltage settling time was measured in order to give an indication of when the transient had essentially ended. As can be seen from the results presented in table III, there was a large variation in the values. This largely random variation is due in part to the change in line voltage distortion caused by phase-controlled switching of parasitic load. The effect of distortion on the steady-state voltage regulation range is discussed in reference 13. As speed and parasitic power vary, voltage distortion varies. Therefore, part of the variation is due to just a change in distortion. Other factors such as changing power factor and alternator load contribute to a voltage regulation range greater than the ± 1 percent goal for the system. Thus the decay of the voltage transient depends on the decay of the frequency transient. And, as will be shown in the following section, the response of frequency varied significantly over the range of useful-load transients.

Frequency Transients

The following terms are defined with the aid of figure 12:

$\frac{F + F_P}{1200} \times 100$	maximum (or minimum) frequency, percent of rated
F	initial operating frequency, Hz
F_P	peak frequency excursion during the transient, Hz
F_F	steady-state frequency difference between load points, Hz
T_R	frequency recovery time: the time for the frequency to come and remain within ± 2 hertz of the final operating frequency, sec
T_P	time to first peak, sec
F_D	damped natural resonant frequency, $1/2 \Delta T$, sec^{-1}
ΔT	time difference between the first peak and the succeeding undershoot, sec

The steady-state frequencies as a function of useful load are plotted in figure 13. The frequency regulation range of 25 hertz was established for reasons given in the next section on the stability of the system. The curves for the 1.0 and 0.85 power factors

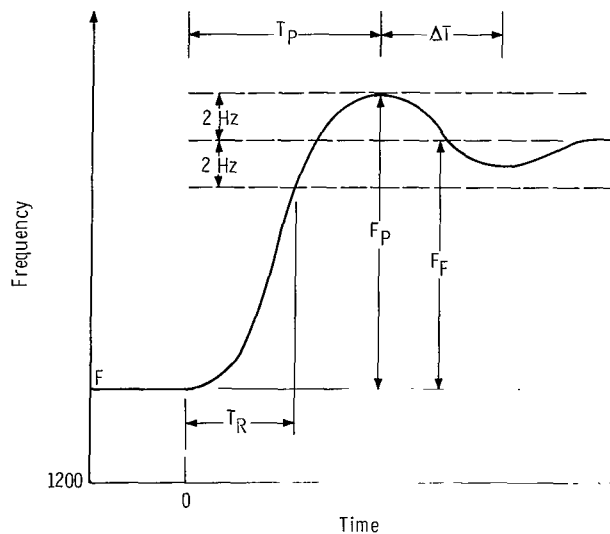


Figure 12. - Definition of parameters used in describing frequency transients.

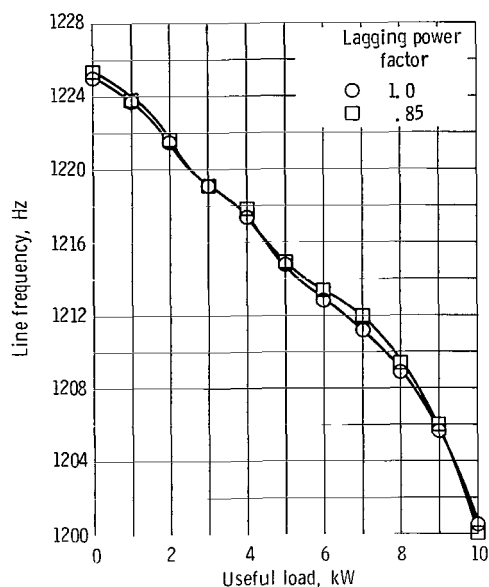


Figure 13. - Line frequency for useful loads at 1.0 and 0.85 (lagging) power factors.

differ primarily as a result of an uncontrolled change in the cold plate temperature. Further discussion of this effect is given in reference 13.

The maximum and minimum transient frequencies obtained for useful-load transients are shown in figure 14. The slight differences between the 1.0- and 0.85-power-factor curves are due to the shift in the speed control characteristic caused by the change in cold plate temperature. The curves essentially define a frequency operating region. For a load application of 8 kilowatts, at 0.85 power factor, the minimum frequency obtained is 100.6 percent of rated. For this load removal, the maximum frequency obtained was 102.2 percent of rated. The frequency settled out at 1225 hertz (102.08 percent of rated) for any load removal. (This frequency exceeds the 2 percent design goal and it will be discussed below.) The variation in the peak frequency attained is due to the nonlinear characteristics of the control system.

The minimum frequency obtained for transient and steady-state conditions was 100.02 percent of rated. The maximum frequency obtained was 102.24 percent of rated. This operating band was considered to be satisfactory.

Frequency recovery time was defined as the time for the frequency to enter and remain within ± 2 hertz of the final frequency. This ± 2 -hertz band was specified to be the maximum allowable modulation in the system. And thus the band served as a reference

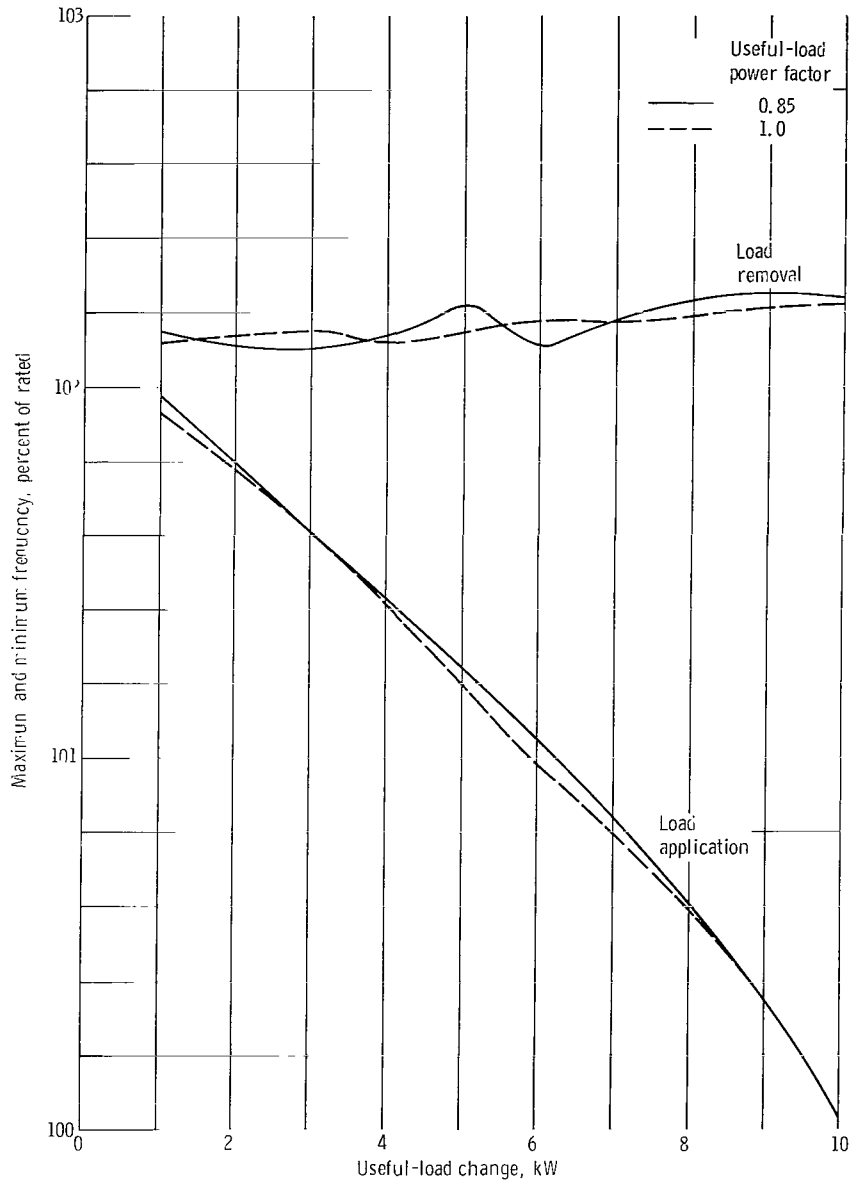
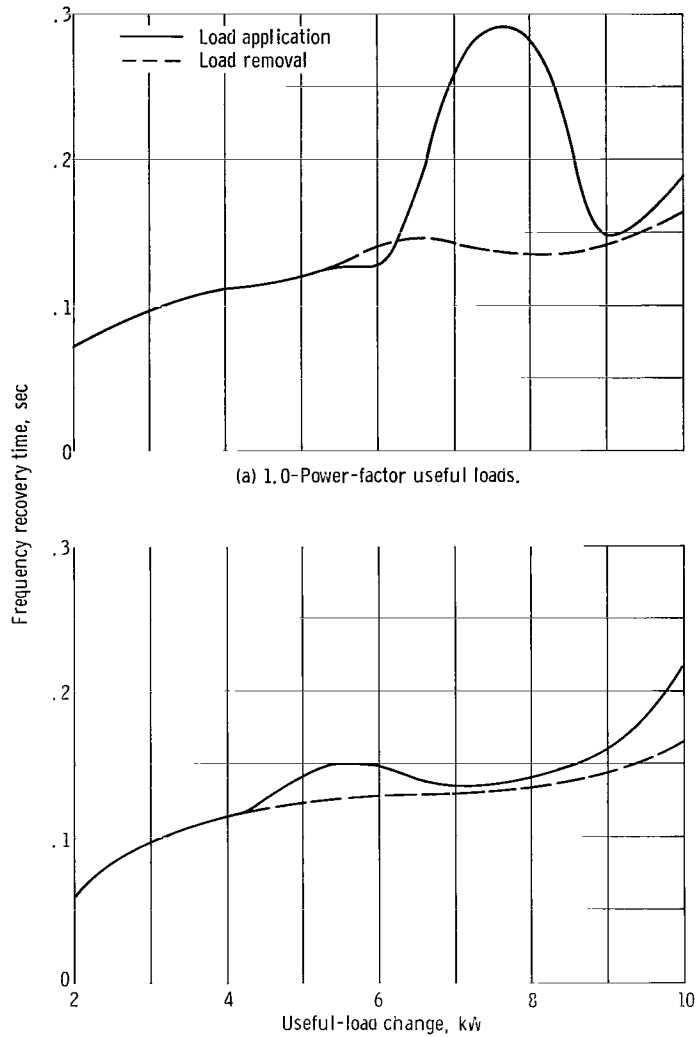


Figure 14. - Maximum and minimum frequency for step useful-load changes.

in the definition. But it was found that in the system tested, the frequency modulation did not exceed ± 0.25 hertz, and this value was barely discernible.

The values of recovery time obtained are plotted in figure 15. For a load application of 7 and 8 kilowatts, at 0.85 power factor, the frequency undershot the ± 2 -hertz band and thus caused the higher-than-average recovery time. The value at 8 kilowatts is about 0.28 second. As will be discussed in the next section, the response of the frequency to various values of loads stepped varied significantly. The response for the 7- and 8-kilowatt load applications was underdamped to the extent that the frequency



(a) 1.0-Power-factor useful loads.
 (b) 0.85-Power-factor (lagging) useful loads.
 Figure 15. - Frequency recovery time for step useful-load changes.

undershoot was greater than the band used for the definition of the recovery time. The response to the 10-kilowatt load application was overdamped.

The values of recovery time obtained are well within the 1-second design goal.

Stability

In order to relate the response of frequency to the standard form used in the analysis

of second-order systems, the following definition is made with reference to figure 12:

$$\frac{F_P - F_F}{F_F} \quad \text{relative overshoot (or undershoot)}$$

The stability of the frequency is related to the relative overshoot. Increasing overshoot means that the response is becoming more oscillatory. Therefore, the overshoot is an indication of the stability of the system. The overshoot to be obtained can be set by adjustment of the speed controller gain.

All useful-load applications were performed with initially no useful load. Therefore, the frequency was initially at its maximum steady-state value. The load application caused the frequency to decrease and in some cases undershoot its final steady-state value. The subsequent removal of useful load caused the frequency to return to its maximum steady-state value and, in some cases, to overshoot this final value. In the following discussion, only the useful-load application case is considered since the initial conditions for each load application were identical.

The relative undershoot of frequency for step application of useful load is given in figure 16. In a linear system there would be no variation in the relative undershoot with

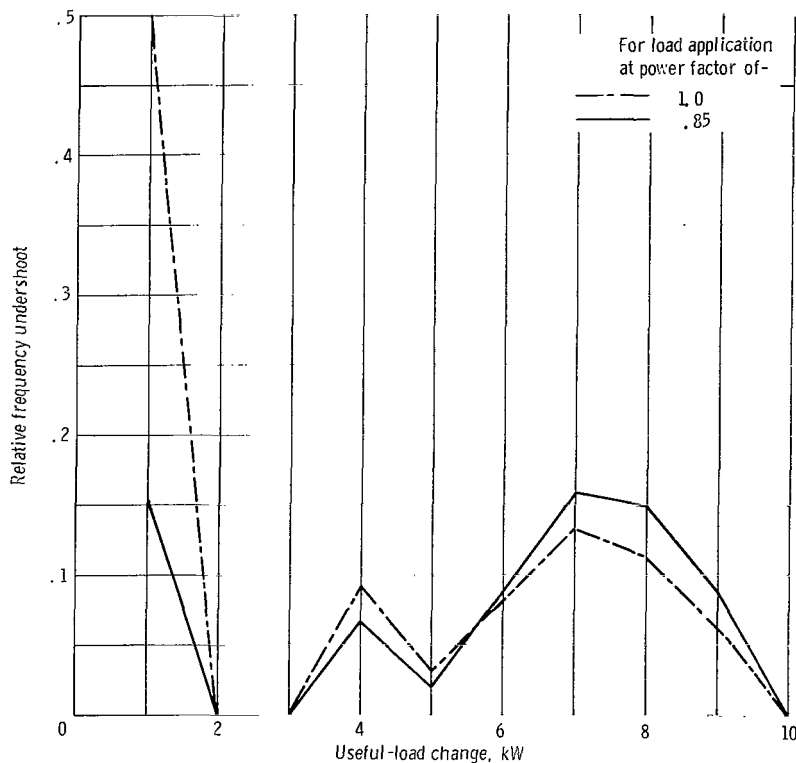


Figure 16. - Relative frequency undershoot for step useful-load changes.

different magnitudes of useful load applied. But this system was nonlinear. The principal contributor to this nonlinearity was the speed controller.

Because of the nonlinearity inherent in the speed controller, the gain varies significantly with frequency. Approximate values of speed controller gain are given in figure 17; they were obtained in the following manner: Since, for the steady-state regulation characteristic of figure 13 (neglecting losses),

$$\text{Parasitic load} = \text{Total load} - \text{Useful load}$$

or

$$\text{PL} = \text{Constant} - \text{UL}$$

then

$$\text{Gain} = K = \left| \frac{\Delta \text{PL}}{\Delta F} \right| = \left| \frac{\Delta \text{UL}}{\Delta F} \right|$$

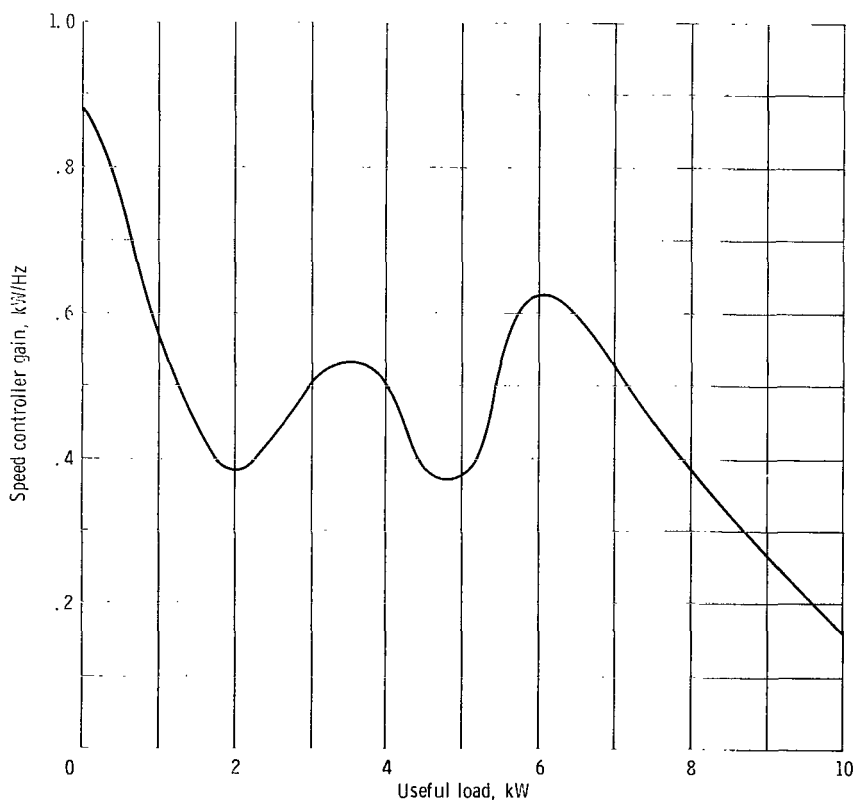


Figure 17. - Incremental gain of speed controller, 1.0-power-factor case. Total steady-state alternator output power, 10.7 kilowatts.

Values of gain about a steady-state operating point were calculated from figure 13. As an illustration, in calculating the gain about the 8-kilowatt, 1.0-power-factor useful-load operating point, ΔF was determined between 7.5 and 8.5 kilowatts useful load giving

$$K = \frac{1 \text{ kW}}{2.6 \text{ Hz}} = 0.38 \text{ kW/Hz}$$

Thus the values of gain are approximate. But the values are another measure of the stability of the frequency. Initial operation of the test system showed that a speed controller gain of $K \geq 1.8 \text{ kW/Hz}$ would cause a continuous oscillation (limit cycle) in the frequency. For the curve in figure 13 the largest value of gain occurred near the zero useful load operating point. The gain about this operating point is approximately 0.9 kW/Hz . This was considered to be adequately low gain for avoiding limit cycles. A 1200- to 1212-hertz frequency control range had been selected as a design goal. Since the incremental gain of the speed controller was then high enough to obtain limit cycles, the controllers were retuned for a 1200- to 1225-hertz control range. This larger control range meant that the +2 percent transient frequency excursion goal was always exceeded.

Since the response of the frequency depends on the gain of the speed controller, there is some correlation between figures 16 and 17. But due to the nonlinearities in the system only a rough correlation is possible. An inspection of the figures reveals that the undershoot depends to some extent on the gain near the final steady-state operating point. The gain of 0.15 kW/Hz near the 10-kilowatt point is so low that no undershoot results for a 10-kilowatt vehicle load application. Between these two values a trend is evident, but no direct correlation between gain and undershoot can be made. Values of T_P (time to first peak) and F_D (damped natural resonant frequency) for each transient performed are given in table IV. The variation in these parameters further illustrates the nonlinearity inherent in the system.

The system is stable when the speed controller is tuned for the 1200- to 1225-hertz steady-state regulation band.

Parasitic Power Margin

In order to maintain control of speed, some value of parasitic load must always be applied over the entire frequency excursion range. Should the speed undershoot the control range, a change in turbine efficiency could cause the speed to continually drop. The value of parasitic load required to maintain speed for rated load application is termed "margin." The margin required for the test system was determined experimentally. Since the response of frequency to a rated load application was overdamped, an arbitrarily small power margin (about 20 W) was sufficient to maintain control of speed.

TABLE IV. - TIME TO FIRST PEAK AND DAMPED NATURAL
 FREQUENCY OF FREQUENCY TRANSIENTS FOR
 STEP USEFUL-LOAD CHANGES

Power factor	Useful load, kW	Load application		Load removal	
		Time to first peak, sec	Damped natural frequency, sec ⁻¹	Time to first peak, sec	Damped natural frequency, sec ⁻¹
1.0	1	0.156	2.5	0.153	4.0
	2	(a)	(a)	.207	2.4
	3	(a)	(a)	.232	3.2
	4	.259	(b)	.215	2.6
	5	.356	1.3	.211	3.4
	6	.318	1.8	.219	3.6
	7	.267	2.9	.213	2.9
	8	.246	1.4	.224	2.8
	9	.232	(b)	.231	3.0
	10	(a)	(a)	.252	3.0
0.85	1	0.198	(b)	0.151	(b)
	2	(a)	(a)	.210	2.7
	3	(a)	(a)	.239	3.1
	4	.239	1.2	.224	2.9
	5	.336	(b)	.227	3.2
	6	.256	2.5	.226	3.2
	7	.253	1.6	.230	2.9
	8	.233	(b)	.233	3.1
	9	.239	(b)	.237	3.1
	10	(a)	(b)	.260	3.2

^aFor this case the response was either critically damped or over-damped.

^bFor this case there was no measurable oscillation.

Startup

The test was performed in the following manner: The proportional air inlet valve was set for an alternator output power of 10.7 kilowatts. No useful load was applied. The on-off valve was then closed and the machine coasted down to zero speed. Finally, the on-off valve was opened. The curves of voltage, speed, and field currents obtained from oscillograph traces are shown in figure 18.

As the speed increases, the residual magnetism of the alternator rotor generates an

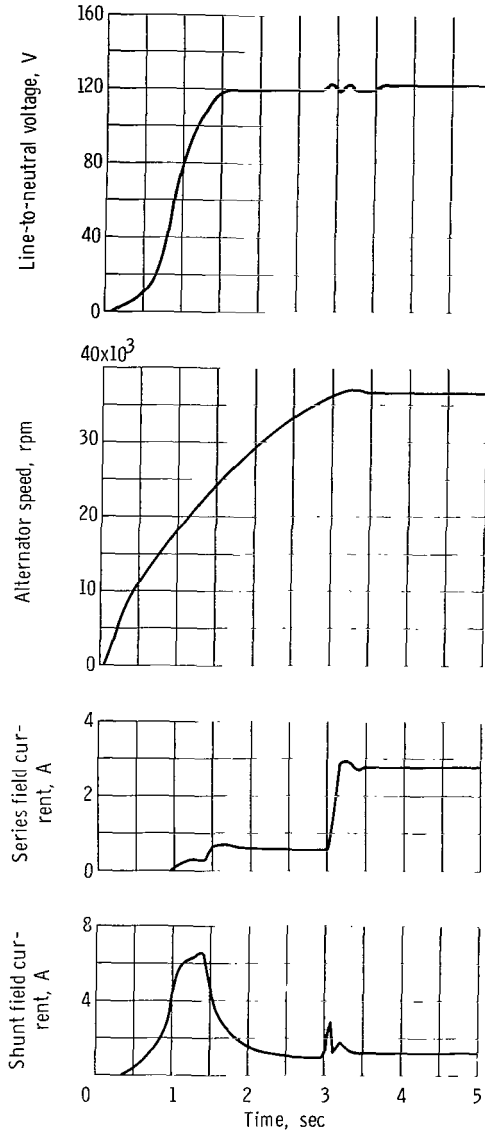


Figure 18. - Startup - response to a step opening of the turbine inlet valve.

increasing voltage. At a generated voltage of 6 volts, the shunt field current increases with line voltage until the current limit circuit in the voltage regulator starts to function. As the line voltage enters the regulation range, the shunt field current decreases to its steady-state operating range. Line voltage has built up to near its rated value at about 26 000 rpm.

The initial series field current is caused by line current supplying the shunt field regulator and the capacitive load of the parasitic load filter. This filter is used to smooth the voltage distortion caused by phase-controlled firing of parasitic load (ref. 13).

The sudden increase in current to about 3 amperes is caused by the speed controller turning on. Effects of the speed achieving the control range are also noticed on the line voltage and on the shunt field current. The addition of the parasitic load stops the acceleration of the rotating unit. Steady-state conditions are achieved in about 3.5 seconds. The main features of this test are that the system built up on residual magnetism and that the controls responded quickly enough to allow only a 0.56 percent speed overshoot.

A typical value of voltage at rated speed resulting from residual magnetism of the alternator during this testing program was 27 volts. Since it had been determined from separate voltage regulator testing that the voltage would build up to 120 volts at rated speed with a generated voltage of 6 volts or greater, no attempt was made to vary the residual magnetism.

SUMMARY OF RESULTS

The performances of the voltage regulator and the parasitic speed controller during step changes in useful load and during a startup were evaluated. The following experimental results were obtained:

1. Voltage transients - The maximum voltage of 123 percent of rated voltage was obtained for rated useful-load removal. For rated useful-load application, the minimum voltage was 81.5 percent. The voltage recovery time did not exceed 0.074 second over the range of useful-load transients. The voltage settling time varied from 0.1 to 0.4 second and was found to depend on the decay of the frequency transient.

2. Frequency transients - Stable operation of the speed controller was obtained over the 1200- to 1225-hertz control range. The maximum incremental gain over this operating range was about 0.9 kW/Hz. The maximum value of frequency recovery time was 0.28 second. Due to the nonlinearity of the speed controller, the response of frequency to step useful-load changes ranged from highly underdamped to overdamped.

3. Margin - Since the response of frequency to step application of rated useful load was overdamped, a parasitic power margin of 20 watts was sufficient to maintain test system speed.

4. Startup - A full-power startup was performed relying on residual magnetism of the alternator. With a residual magnetism large enough to generate about 27 volts at rated speed, the test system built up to rated conditions in 3.5 seconds with only a 0.56 percent speed overshoot.

Lewis Research Center,
National Aeronautics and Space Administration,
Cleveland, Ohio, June 25, 1970,
120-27.

REFERENCES

1. Klann, John L.: 2 to 10 Kilowatt Solar or Radioisotope Brayton Power System. Intersociety Energy Conversion Engineering Conference. Vol. 1. IEEE, 1968, pp. 407-415.
2. Anon.: Electrical Control Package for Brayton Power Conversion System. Hayes International Corp. (NASA CR-72497), Jan. 1969.
3. Lalli, V. R.: Sunflower Rotational Speed Control Topical Report. Rep. ER-4947, Tapco Div., Thompson Ramo Wooldridge, Inc. (NASA CR-50802), Mar. 1963.
4. Dauterman, W. E.: Snap-2 Power Conversion System. Model 6 Two-Phase Flight-Packaged Speed Control. Rep. ER-5908, Thompson Ramo Wooldridge, Inc. (AEC No. NAA-SR-6319), June 1964.
5. Nice, A. W.; and Bradley, S. L.: SNAP-8 Electrical System. IEEE Trans. on Aerospace, vol. AS-2, no. 2, Apr. 1964, pp. 867-873.
6. Word, John L.; Fischer, Raymond L. E.; and Ingle, Bill D.: Static Parasitic Speed Controller for Brayton-Cycle Turboalternator. NASA TN D-4176, 1967.
7. Fischer, Raymond L. E.; and Droba, Darryl J.: Dynamic Characteristics of Parasitic-Loading Speed Controller for 10-Kilowatt Brayton Cycle Turboalternator. NASA TM X-1456, 1968.
8. Corcoran, Charles S.; and Yeager, LeRoy J.: Summary of Electrical Component Development for a 400-Hertz Brayton Energy Conversion System. NASA TN D-4874, 1968.
9. Valgora, Martin E.; and Perz, Dennis A.: Steady-State Electrical Performance of a 400-Hertz Brayton Cycle Turboalternator and Controls. NASA TN D-5658, 1970
10. Repas, David S.; and Edkin, Richard A.: Performance Characteristics of a 14.3-Kilovolt-Ampere Modified Lundell Alternator for 1200 Hertz Brayton-Cycle Space-Power System. NASA TN D-5405, 1969.
11. Dunn, James H.: The 1200-Hertz Brayton Electrical Research Components. Rep. APS-5286-R, AiResearch Mfg. Co. (NASA CR-72564), Mar. 19, 1969.
12. Ingle, B. D.; and Corcoran, C. S.: Development of a 1200-Hertz Alternator and Controls for Space Power Systems. Intersociety Energy Conversion Engineering Conference. Vol. 1. IEEE, 1968, pp. 438-447.

13. Ingle, Bill D.; Wimmer, Heinz L.; and Bainbridge, Richard C.: Steady-State Characteristics of a Voltage Regulator and a Parasitic Speed Controller on a 14.3-Kilovolt-Ampere, 1200-Hertz Modified Lundell Alternator. NASA TN D-5924, 1970.
14. Perz, Dennis A.: Method for Measuring Alternator Voltage Transients. NASA Tech Brief 68-10513, Nov. 1968.
15. D'Azzo, John J.; and Houpis, Constantine H.: Feedback Control System Analysis and Synthesis. Second ed., McGraw-Hill Book Co., Inc., 1966.
16. Gilbert, Leonard J.: Reduction of Apparent-Power Requirement of Phase-Controlled Parasitically Loaded Turboalternator by Multiple Parasitic Loads. NASA TN D-4302, 1968.

FIRST CLASS MAIL



POSTAGE AND FEES PAID
NATIONAL AERONAUTICS AND
SPACE ADMINISTRATION

08U 001 28 51 3DS 70272 00903
AIR FORCE WEAPONS LABORATORY /WLOL/
KIRTLAND AFB, NEW MEXICO 87117

ATT E. LOU BOWMAN, CHIEF, TECH. LIBRARY

POSTMASTER: If Undeliverable (Section 158
Postal Manual) Do Not Return

"The aeronautical and space activities of the United States shall be conducted so as to contribute . . . to the expansion of human knowledge of phenomena in the atmosphere and space. The Administration shall provide for the widest practicable and appropriate dissemination of information concerning its activities and the results thereof."

— NATIONAL AERONAUTICS AND SPACE ACT OF 1958

NASA SCIENTIFIC AND TECHNICAL PUBLICATIONS

TECHNICAL REPORTS: Scientific and technical information considered important, complete, and a lasting contribution to existing knowledge.

TECHNICAL NOTES: Information less broad in scope but nevertheless of importance as a contribution to existing knowledge.

TECHNICAL MEMORANDUMS: Information receiving limited distribution because of preliminary data, security classification, or other reasons.

CONTRACTOR REPORTS: Scientific and technical information generated under a NASA contract or grant and considered an important contribution to existing knowledge.

TECHNICAL TRANSLATIONS: Information published in a foreign language considered to merit NASA distribution in English.

SPECIAL PUBLICATIONS: Information derived from or of value to NASA activities. Publications include conference proceedings, monographs, data compilations, handbooks, sourcebooks, and special bibliographies.

TECHNOLOGY UTILIZATION PUBLICATIONS: Information on technology used by NASA that may be of particular interest in commercial and other non-aerospace applications. Publications include Tech Briefs, Technology Utilization Reports and Notes, and Technology Surveys.

Details on the availability of these publications may be obtained from:

SCIENTIFIC AND TECHNICAL INFORMATION DIVISION
NATIONAL AERONAUTICS AND SPACE ADMINISTRATION
Washington, D.C. 20546